

Article

Spatiotemporal Characteristics of Drought in Northwest China Based on SPEI Analysis

Yongqin Peng ^{1,*}, Tao Peng ² and Yan Li ¹

¹ Chongqing Southwest Research Institute for Water Transport Engineering, Chongqing Jiaotong University, Chongqing 400016, China

² Chongqing Gangli and Carbon Environmental Technology Co., Ltd., Chongqing 400016, China

* Correspondence: 98000000909@cjtu.edu.cn

Abstract: Drought has a direct impact on regional agricultural production, ecological environment, and economic development. The northwest region of China is an important agricultural production area, but it is also one of the most serious areas of water shortage due to drought and little rain. It is of great significance to make full use of agricultural resources to clarify the temporal and spatial distribution characteristics of the drought regime in Northwest China. Based on the Standardized Precipitation Evapotranspiration Index (SPEI), this paper used the methods of Mann–Kendall non-parameter trend, mutation test, and Morlet wavelet analysis to explore the drought characteristics in Northwest China from 1961 to 2017. The results showed that the spatial distribution of SPEI on annual and seasonal scales differed slightly in different regions, but from northwest to southeast, the distribution was generally wetter to drier. The drought intensity (S_{ij}) had a step-like distribution with a range of 1.14–1.98. Based on S_{ij} analysis, the frequency of drought in Northwest China was moderate, followed by extreme drought, severe drought, and light drought. The inter-annual drought station proportion (P_j) ranged from 7.4% to 84.1%. A total of 25, 18, 7, and 5 years of pan-regional drought, regional drought, partial region drought, and local drought occurred, respectively, based on P_j analysis. Moreover, from the whole study period, the regional drought changes tended to cause humidification to different degrees. The results of Morlet wavelet analysis showed that there were multiple time scales of 33–52, 11–19, and 4–7 years of SPEI in the entire time domain, and dry and wet trends occurred. The results of the present research can provide a reference for the efficient utilization of water resources, drought monitoring and early warning, drought prevention, and drought relief in Northwest China.

Keywords: drought index; SPEI; climate inclination rate; northwest China; wavelet analysis



Citation: Peng, Y.; Peng, T.; Li, Y. Spatiotemporal Characteristics of Drought in Northwest China Based on SPEI Analysis. *Atmosphere* **2023**, *14*, 1188. <https://doi.org/10.3390/atmos14071188>

Academic Editors: Zhiqiang Gong, Gang Huang and Chao Li

Received: 20 June 2023

Revised: 15 July 2023

Accepted: 21 July 2023

Published: 23 July 2023



Copyright: © 2023 by the authors. Licensee MDPI, Basel, Switzerland. This article is an open access article distributed under the terms and conditions of the Creative Commons Attribution (CC BY) license (<https://creativecommons.org/licenses/by/4.0/>).

1. Introduction

Drought occurs widely in the world. Drought often causes serious losses and has an important impact on regional agricultural production, the ecological environment, and economic development [1,2]. Previous research proves that climate warming is currently a matter of global environmental concern [3]. Due to the influence of global warming, the climate and environment have also undergone many changes, and drought disasters have occurred frequently. Under the current environmental background, it is urgent to research drought disasters. However, due to the time variability, space variability, complex physical processes, and non-structural characteristics of drought, research on the identification and characterization of drought faces severe challenges. Hence, a correct understanding of the spatiotemporal characteristics of drought is of great significance for drought disaster assessment and disaster prevention and reduction [4].

A large number of domestic and foreign scholars have conducted quantitative research on drought using the drought indexes of standardized precipitation index (SPI) [5], palmer drought severity index (PDSI) [6], and standardized precipitation evapotranspiration index

(climate inclination rate) [7,8]. Among them, SPI is a drought index based on precipitation, but it does not consider the correlation between other meteorological variables (e.g., temperature, wind, and relative humidity) and drought, and there are certain limitations in evaluating drought [5]. Additionally, PDSI fully considers several parameters such as precipitation, runoff, and soil water content that affect regional dry and wet conditions, and the physical mechanism is relatively clear. However, the calculation process of PDSI is complex and requires high-quality regional data [6]. Simultaneously, the evapotranspiration of the PDSI and SPEI indexes can be calculated by the Thornthwaite and Penman-Monteith equations. However, the Thornthwaite equation tends to underestimate evapotranspiration in arid and semiarid regions while overestimating it in humid equatorial and tropical regions [9]. Inversely, the physical mechanism is more explicit, as the Penman-Monteith equation is widely recommended as a standard for calculating evapotranspiration [9]. By synthesizing PDSI's sensitivity to temperature and SPI's advantage of multiple time scales, SPEI can accurately characterize regional dry and wet conditions and their changing trends and has been widely used in regional dry and wet condition analysis in recent years [10–12].

The Northwest area is an important agricultural production area in China, but it is also one of the most vulnerable areas where water resources are short because of little rain [13,14]. At the same time, Northwest China also has the advantages of abundant sunlight and a large daily temperature difference, which are suitable for the production of grain, cotton, and some special products [15–17], and there is a huge agricultural production potential. However, unreasonable irrigation methods and incomplete water conservation facilities lead to lower utilization of water resources [18]. Coupled with the continuous expansion of agricultural sowing areas in recent years, agricultural water consumption has increased in Northwest China [19]. The shortage of water resources has become the main factor restricting economic development in Northwest China [20]. To alleviate the contradiction between the supply and demand of water resources in all aspects of society, it is of important practical significance to allocate water resources more reasonably.

In this paper, the methods of Mann–Kendall non-parameter trend, mutation test, and Morlet wavelet analysis were simultaneously used, and the SPEI index was calculated. The objectives of this study were to (1) reveal the distribution of the climate tendency rate of SPEI; (2) clarify the drought frequency at SPEI annual scale; and (3) analyze the spatiotemporal evolution characteristics of drought in Northwest China. The research results provide a theoretical basis and technical support for the efficient utilization of water resources, drought monitoring and early warning, drought prevention, and drought relief in Northwest China.

2. Overview and Explanation of Data

2.1. Overview of the Study Area

The research area of this paper is Northwest China (Figure 1), including the whole of the Xinjiang Uygur Autonomous Region, Qinghai Province, Gansu Province, the Ningxia Hui Autonomous Region, and Shaanxi Province. The latitude and longitude range is 73°25' E–111°19' E and 31°35' N–49°15' N. The region is characterized by BWk according to the Köppen–Geiger climate classification system. The area of Northwest China is largely surrounded by high mountains and is difficult to reach by moist ocean currents, making it the driest region in China. In addition, the region has a harsh climate, a fragile environment, scarce vegetation, and limited evaporation of water vapor from the ground. The spatiotemporal inhomogeneity of precipitation and the frequency and intensity of extreme drought events increase significantly due to climate warming [21]. Most of the precipitation is concentrated in the non-agricultural high mountainous area. While precipitation in a dry-farming region, which relies mainly on natural precipitation for agricultural production, is very low. As a result, most of the region is an irrigated farming area, which is severely restricted by irrigation conditions.

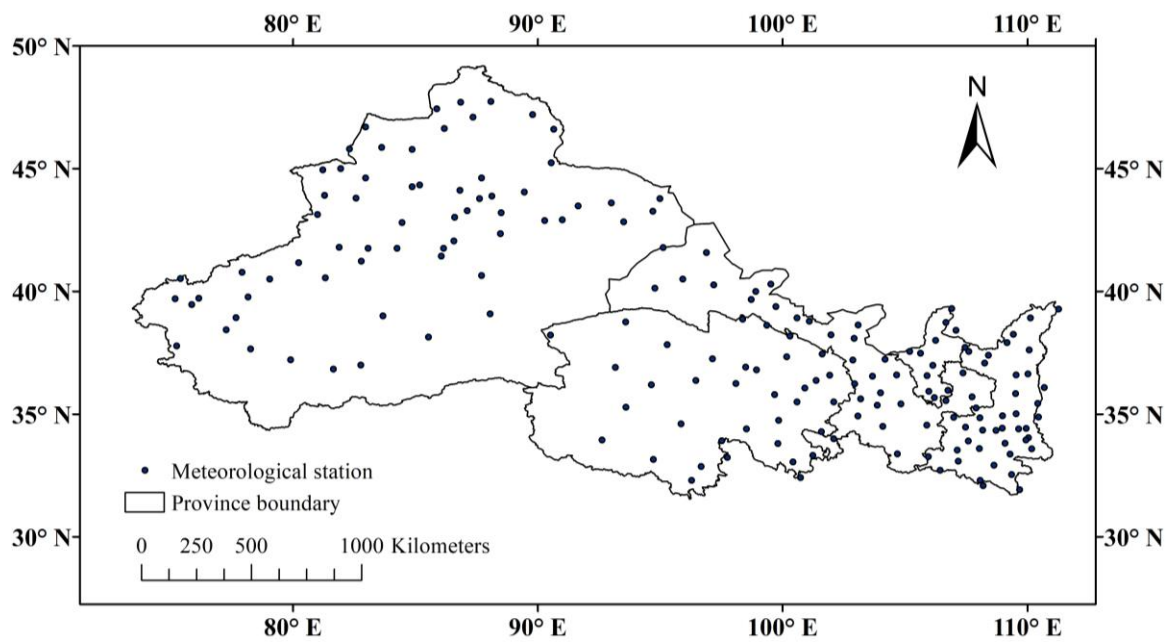


Figure 1. Study area and distribution map of studied weather stations.

2.2. Data Sources

In this paper, the daily meteorological data of 176 meteorological stations from 1961 to 2017 were obtained from the China Meteorological Data Network (<http://data.cma.cn/> accessed on 17 May 2021). The daily meteorological data included average wind speed, average temperature, maximum temperature, minimum temperature, sunshine hours, average relative humidity, precipitation, etc.

2.3. Research Methods

2.3.1. Standardized Precipitation Evapotranspiration Index (SPEI)

The calculation of SPEI was divided into four steps, which are detailed in the reference [22]. Firstly, the difference (D) between precipitation (P) and potential evapotranspiration (ET_0) was calculated as follows:

$$D = P - ET_0 \tag{1}$$

Here, in order to consider both temperature and aerodynamic factors, ET_0 was calculated by Penman–Monteith formula.

Then, the accumulation sequence of water surplus and deficit on different time scales for climatology was established:

$$D_n^k = \sum_{i=0}^{k-1} (P_{n-1-i} - ET_{0\ n-1-i}), n \geq k \tag{2}$$

where n is the number of computations; k is the time scale of the calculation.

The log-logistic probability density function with three parameters was used to fit Equation (2):

$$f(x) = \frac{\beta}{\alpha} \left(\frac{x - \gamma}{\alpha} \right)^{\beta-1} \left[1 + \left(\frac{x - \gamma}{\alpha} \right)^\beta \right]^{-2} \tag{3}$$

where $f(x)$ is the probability density function; α , β , and γ are the scale parameter, shape parameter, and origin parameter, respectively, which can be estimated by the linear moment method. Then, the cumulative probability function $F(x)$ was calculated as follows:

$$F(x) = \left[1 + \left(\frac{x - \gamma}{\alpha} \right)^\beta \right]^{-1} \tag{4}$$

Lastly, the sequence was transformed into a standard normal distribution to obtain the corresponding SPEI:

$$\text{SPEI} = W - \frac{C_0 + C_1W + C_2W^2}{1 + d_1W + d_2W^2 + d_3W^3} \tag{5}$$

where, $W = \sqrt{-2 \ln(P)}$; when $P \leq 0.05$, $P = 1 - F(x)$; when $P > 0.05$, $P = 1 - P$, and the symbol of SPEI is reversed. Here, $C_0 = 2.515517$, $C_1 = 0.802853$, $C_2 = 0.010328$, $d_1 = 1.432788$, $d_2 = 0.189269$, $d_3 = 0.001308$.

2.3.2. Interpolation Calculation of P and ET_0

The calculation of ET_0 was mainly divided into the following three aspects:

- (1) If less data was missing, two conditions existed. When the missing sequencing column was less than 5d, the linear interpolation of recent days' data was used to interpolate. When $5d < \text{missing sequencing column} < 30d$, the multi-year average of the same day was used to interpolate [23]. Here, the Penman–Monteith formula (ET_{0PM}) was also used to calculate the ET_0 [24].
- (2) If longer series data were missing, the Penman–Monteith formula cannot be used. By this time, the ET_0 can be calculated using the formula ET_{0D} provided by FAO56 based on the absence of sunshine hours, relative humidity, and/or wind speed [24]. Firstly, the ET_{0PM} and ET_{0D} sequences were obtained by using the two formulas. Then, Equation (7) was obtained by linear fitting, and the ET_0 was calculated accordingly.

$$ET_{0D} = 0.0023(T_{mean} + 17.8) (T_{max} - T_{min})^{0.5} R_a \tag{6}$$

$$ET_{0PM} = b + a \cdot ET_{0D} \tag{7}$$

- (3) According to the geographical similarity hypothesis, the closer the geographical distance, the more similar the meteorological conditions of the stations. The interpolation processing of the data was carried out in our study.

If the data of the station was missing for many years and the ET_0 cannot be calculated by using step (2), the ET_0 was calculated by using the existing data of the current station first. Additionally, the ET_{0a} of the stations with adjacent or similar conditions that were consistent with the corresponding years of the site was calculated. Finally, the linear relationship between ET_{0a} and ET_0 was analyzed. The ET_0 of the current station was interpolated by Equation (8).

$$ET_0 = b + a \cdot ET_{0a} \tag{8}$$

If the precipitation of the station was missing for many years, the ET_0 , $P^{1/3}$, $T_{mean}^{1/3}$, and RH_{mean} of the stations with adjacent or similar conditions that were consistent with the corresponding years of the site were calculated [25,26]. Then, the multivariate linear relationship between ET_0 , $P^{1/3}$, $T_{mean}^{1/3}$, and RH_{mean} with $P_0^{1/3}$ existed. By that time, the missing precipitation of the station can be restored according to the following equation.

$$P_0^{1/3} = b + a_1 \cdot ET_0 + a_2 \cdot P^{1/3} + a_3 \cdot T_{mean}^{1/3} + a_4 \cdot RH_{mean} \tag{9}$$

2.3.3. Spatiotemporal Analysis of Drought Index Climate Tendency Rate

The linear regression equation between X and t was established by using X to represent the sequence values of climate elements and t to represent the corresponding time.

$$X = b_0 + b_1t \tag{10}$$

where, b_0 is the intercept of the equation; b_1 is the regression coefficient. The climate tendency rate of the climate factor is 10 times b_1 .

Drought Evaluation Index Calculation

In our study, drought characteristics were evaluated by the drought frequency (P_i), drought intensity (S_{ij}), and drought station proportion (P_j).

- (1) The P_i was used to evaluate the frequency of drought in a station during the years with available data, which was calculated by the following equation:

$$P_i = \frac{n}{N} \times 100\% \tag{11}$$

where N is the number of years for which valid meteorological data exists at a station; n is the number of years in which drought occurred at a station.

- (2) The S_{ij} was used to evaluate the severity of drought occurring in a region, which was calculated as follows:

$$S_{ij} = \frac{1}{m} \sum_{i=1}^m |SPEI_i| \tag{12}$$

where m is the number of stations where drought occurs; $|SPEI_i|$ is the absolute value of $SPEI$ at a station when drought occurs. Then, regional drought intensity can be divided into four levels according to Huang et al. [27], as shown in Table 1.

Table 1. Definition of drought degree.

Drought Intensity (S_{ij})		Drought Station Proportion (P_j)	
S_{ij}	Drought grade	P_j	Drought range
$2 \leq S_{ij}$	Extreme drought	$50\% \leq P_j$	Pan-regional drought
$1.5 \leq S_{ij} \leq 2$	Severe drought	$33\% \leq P_j \leq 50\%$	Regional drought
$1 \leq S_{ij} \leq 1.5$	Moderate drought	$25\% \leq P_j \leq 33\%$	Partial regional drought
$0.5 \leq S_{ij} \leq 1$	Light drought	$10\% \leq P_j \leq 25\%$	Local drought
$0.5 \leq S_{ij}$	No drought	$10\% \leq P_j$	Non-obvious drought

- (3) The P_j was used to evaluate the size of the influence area of drought, which was calculated by the proportion of the number of drought stations in the total number of stations.

$$P_j = \frac{m}{M} \times 100\% \tag{13}$$

where m is the number of stations where drought occurred; M is the total number of meteorological stations. Then, regional drought intensity can be divided into five levels based on P_j values referring to Huang et al. [27], as shown in Table 1.

Mann–Kendall Mutation Test

The Mann–Kendall mutation test is a non-parametric statistical test method that is easy to calculate, does not require samples to follow a certain distribution, and is not disturbed

by a few outliers [28]. It has been verified that this method is suitable for the analysis of type variables and sequence variables. Hence, in our study, the M-K method was used to test the drought trend expressed by the annual average SPEI and the four-season annual average SPEI of 176 meteorological stations in Northwest China from 1961 to 2017. The specific calculation process was as follows [2,28,29].

For time series 'x' with sample size 'n', an order column was constructed:

$$s_k = \sum_{i=1}^k r_i \quad (k = 2, 3, \dots, n) \quad (14)$$

when $x_i > x_j$, $r_i = 1$; when $x_i < x_j$, $r_i = 0$. Here, $j = 1, 2, \dots, i$.

The statistics were defined under the assumption that the time series was randomly independent:

$$UF_k = \frac{s_k - \bar{s}_k}{\sqrt{Var(s_k)}} \quad (k = 1, 2, \dots, n) \quad (15)$$

where, $UF_1 = 0$, \bar{s}_k and $Var(s_k)$ is the mean and variance of s_k . If x_1, x_2, \dots, x_n were independent of each other and showed the same continuous distribution, the \bar{s}_k and $Var(s_k)$ were calculated as follows:

$$\begin{cases} \bar{s}_k = \frac{n(n-1)}{4} \\ Var(s_k) = \frac{n(n-1)(2n+5)}{72} \end{cases} \quad (16)$$

UF_i was a sequence of standard normal distribution statistics calculated in the order of the values of x . For a given significant level of α , if $|UF_i| > U_\alpha$, it suggested that 'x' had obvious trend. By the time, $UB_k = -UF_k (k = n, n-1, \dots, 1)$, $UB_1 = 0$. $UF_k \geq 0$ indicated an upward trend, and vice versa. Crossing the critical boundary indicated a significant change. In addition, if the curve is formed by UF_k and UB_k appeared at the intersection of the critical boundary, the corresponding time point was the time when the mutation began.

Wavelet Analysis

Wavelet analysis is widely used for the local analysis of signal time-frequency by analyzing the change of signal time-frequency to highlight some of its characteristics and has the function of time-frequency multi-resolution. It can clearly reveal the change period and the change trend under different time scales in non-stationary time series such as precipitation and temperature and can estimate its future development trend qualitatively and quantitatively. In this paper, by using the built-in function of Matlab R2016b software, the boundary effect was reduced first, and then the wavelet coefficient was calculated by the Morlet complex wavelet [30]. At the same time, the Surfer 14 software (Golden Software, Inc., Golden, CO, USA) was used to draw the contour map of the relevant data, and the wavelet square difference was calculated. Finally, the periodic oscillation characteristics of the regional average annual SPEI index were analyzed.

Spatial Interpolation Method

For the point-to-surface conversion of data such as load, climate tendency rate, and drought frequency, the Kriging method was used to interpolate data [31] from 176 stations in the whole research area combined with the ArcGIS 10.2.2 software, and the relevant spatial distribution map of area distribution was obtained. The condition under which the Kriging method was applicable was that there was spatial variability in the regionalized variables. It was a linear, unbiased, optimal estimation of unknown points based on known station data, considering the position relationship with other unknown points and the structural information provided by the variance function. Meanwhile, it can not only quantify the spatial autocorrelation between known points but also explain the spatial distribution of sampling points in the predicted region.

3. Results and Discussion

3.1. Spatial Distribution of Climate Tendency Rate of SPEI in Northwest China

The spatial distribution of the annual scale and seasonal scale climate tendency rates of SPEI in Northwest China is shown in Figure 2. From the east-west perspective, the SPEI climate tendency rates of all time scales were gradually decreasing from west to east, except for the trend of first decreasing and then increasing from west to east on the winter scale. From the north-south perspective, the SPEI climate tendency rates of all time scales were gradually decreasing from north to south, except for the trend of first decreasing and then increasing from north to south on the winter scale.

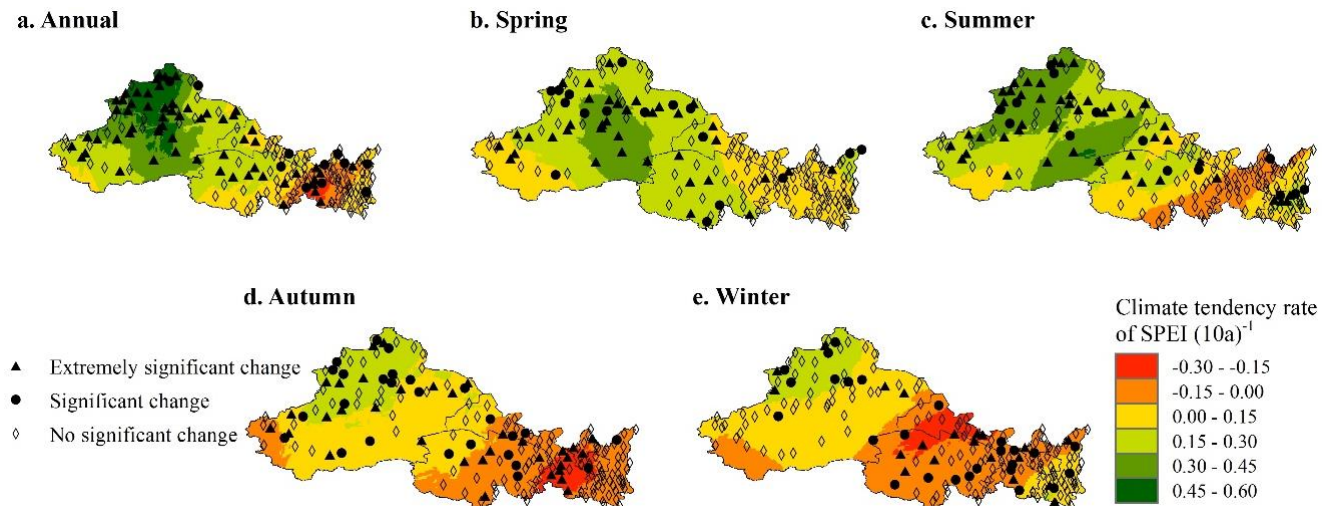


Figure 2. Spatial distribution of climate tendency rate of SPEI on annual and seasonal scales in Northwest China.

From the spatial distribution of the annual SPEI climate tendency rate in Northwest China, the drought trend was gradually changing from wet to dry from northwest to southeast (Figure 2a). Further analysis from the seasonal scale showed that the whole area of Northwest China presented a trend of humidification in spring, and the trend value of humidification gradually decreased from northwest to southeast (Figure 2b). From the spatial distribution of the SPEI climate tendency rate on summer and autumn scales, the trend of SPEI climate tendency in Northwest China was from wet to dry from northwest to southeast, except for a few areas (Figure 2c,d). From the spatial distribution of the SPEI climate tendency rate on the winter scale, Northwest China basically presented an obvious trend from wet to dry and then from dry to wet from northwest to southeast (Figure 2e). In Northwest China, the terrain is complicated, the altitude gap is wide, and the spatiotemporal variability of meteorological elements is large, which leads to the spatial distribution of drought conditions becoming complicated.

3.2. Spatial Analysis of Drought Frequency at SPEI Annual Scale in Northwest China

According to the spatial distribution of drought frequency at the SPEI annual scale in Northwest China (Figure 3), the frequency of moderate drought was the highest, followed by extreme drought, severe drought, and finally light drought. Notably, moderate drought was easy to occur in each region of Northwest China (Figure 3b). The regions with high frequency of extreme drought were mainly distributed in the western and central parts of Northwest China, but less in the eastern part (Figure 3d). The frequency of severe drought was relatively uniform, with a range of 10.0–12.5%, and some other scattered small areas had relatively high or low frequency (Figure 3c). While the spatial distribution of the frequency of light drought was not obvious, the regions with high and low frequencies were scattered (Figure 3a). On the whole, the frequency of light drought in about two-thirds of

the regions was between 10.0% and 12.5%, and the frequency of light drought in one-third of the regions was basically between 5.0% and 7.5%.

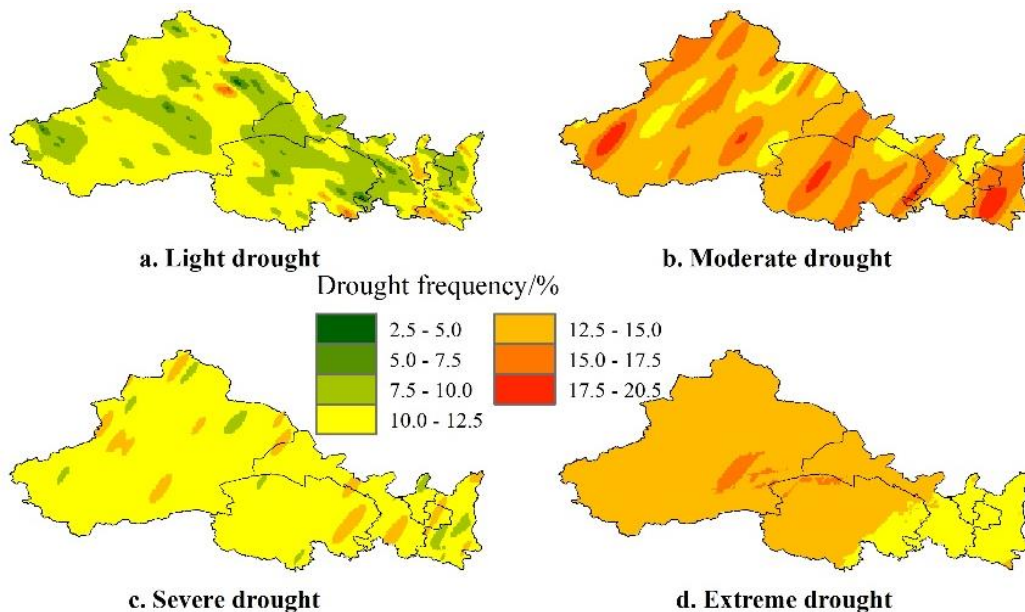


Figure 3. Spatial distribution of different drought degrees in Northwest China.

In summary, the occurrence frequency of different droughts in Northwest China had a relatively obvious regional distribution, which reflected the characteristics of the large variability of meteorological elements. However, as a whole, it can be seen that the central and western regions of Northwest China were mainly characterized by extreme drought and moderate drought, and the probability of various grades of drought was higher in the eastern regions.

3.3. SPEI and Drought Temporal Pattern in Northwest China

3.3.1. Analysis of Annual SPEI and Drought Time Pattern

The annual SPEI index in Northwest China showed a step-like change during 1961–2016 (Figure 4a). First of all, the overall trend of drought was relatively stable, and then it gradually changed to a wetter state and maintained a fluctuating humid state. The results of the present study were similar to those of Zhang et al. [32]. According to the intersection point (mutation point) of the UF and UB curves obtained by the M-K mutation test of the annual SPEI, the whole research period can be divided into two periods: the early dry period (1961–1982) and the late wet period (1983–2016). In the early period, the drought index was negative except for a few years, and the drought phenomenon was generally present. In addition, the later stage was basically wet. After 1992, the UF curve always exceeded the critical threshold of $\alpha = 0.05$, indicating that the trend of moisture increased significantly during this period, but there were also several years of extreme drought. Yang et al. [33] and Liu et al. [34] also obtained similar results. According to the changing trend of SPEI in recent years, it can be seen that the possibility of regional drought will be higher in the future. According to the inter-annual variation of SPEI in different seasons and its M-K mutation test (Figure 4b–e), it can be seen that the four seasons in Northwest China showed a trend of changing from dry to wet, and in recent years, only autumn had become wetter, while other seasons had shown a trend of decreasing wetness. Chen et al. [35] and Cao et al. [12] also draw a similar conclusion. The above research results proved that Northwest China presented a trend of humidification. Numerous studies have indicated that in arid and semiarid regions, water availability is the main factor in vegetation distribution and productivity [12,36]. The increase in rainfall would expand the planting area for agricultural water, and the planting structure may change; meanwhile, the

increase in rainfall is also conducive to ecological restoration [12]. Therefore, humidification in Northwest China would be beneficial to ecological environment construction and social and economic development in the arid area of Northwest China.

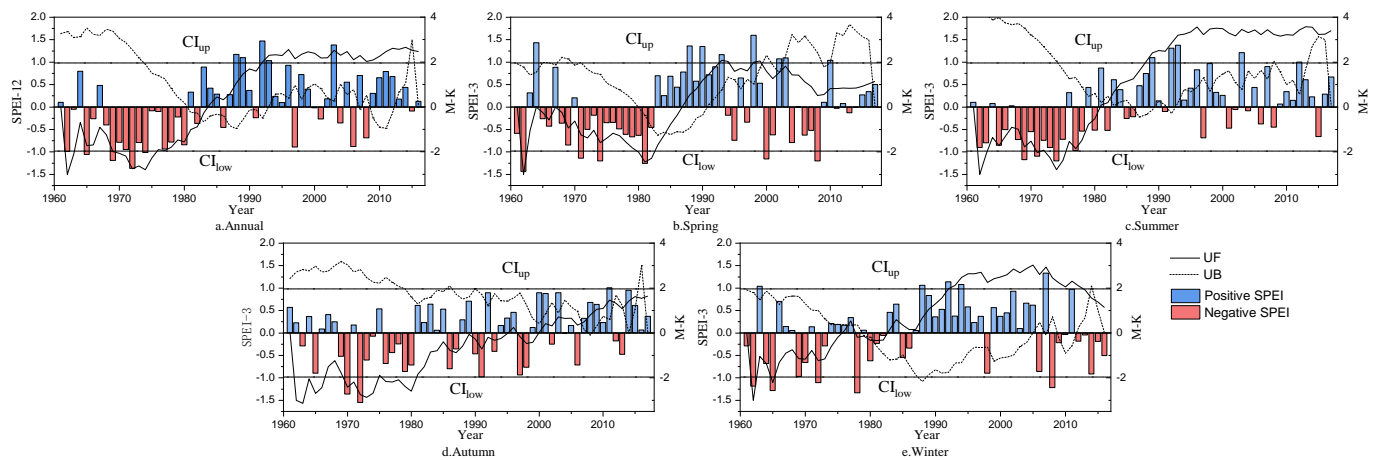


Figure 4. Annual variation of SPEI in annual, spring, summer, autumn, winter, and their M-K test result in Northwest China.

The spring SPEI index showed that the drought situation in Northwest China intensified significantly from 1964 to 1981 and reached a significant level between the late 1970s and early 1980s (Figure 4b). Then, there was a long period of wetness (1983–1993), and finally, a dry and wet alternating period appeared. During this period, extreme drought or wetness occurred. The typical SPEI years were 1998 (1.60), 2000 (−1.16), and 2008 (−1.20). Therefore, on a spring scale, combined with the above analysis results and the mutation point of the M-K mutation, the study period can be divided into three periods: the early dry period (1961–1982), the middle wet period (1983–1996), and the late dry and wet alternating period (1996–2016).

The variation trend of the summer scale was similar to that of the annual scale SPEI, which also showed a step-like change (Figure 4c). According to the intersection of the UF and UB curves, the whole research period can be divided into two periods: the early sustained drought period (1961–1981) and the late alternating drought period (1982–2016). In the early summer, except for a few years, the SPEI index was negative, showing a continuous drought. And, in the late summer, it was alternating between dry and wet, but the overall state was wet.

The SPEI on the autumn scale fluctuated between dry and wet, but the drought trend was more obvious in the first half of the period and the wet trend was dominant in the second half. According to the change in the SPEI index in the summer, Northwest China has tended to be humid in recent years (Figure 4d).

The whole period of winter showed a gradually wetter trend, but in recent years, the wetness trend has been gradually decreasing, and there may be an obvious drought situation (Figure 4e). According to the intersection of the UF and UB curves, the whole period can be divided into two periods: the early dry period (1961–1980) and the late wet period (1981–2016). In the early period, the drought situation gradually eased and in the later period, it was basically in a humid state, but at the end of the last period, the drought situation appeared. However, Liu et al. [34] found the abrupt change points of meteorological drought in spring, summer, autumn, and winter in Northwest China were 1982, 1975, 1998, and 1980, respectively, by using the Pettitt test method. The different conclusions drawn by different researchers may be due to the different research methods, the length of data collection, and the number of sites.

According to the inter-annual changes in drought intensity and drought station proportion (P_i) represented by the annual SPEI in Northwest China (Figure 5), there were obvious inter-annual differences in drought intensity, and the drought intensity had a step-like

distribution on the whole, which corresponded to the variation of the regional drought index on its annual scale. Before 1979, it was a relatively high drought intensity, ranging from 1.4 to 1.98, which varied between moderate drought and severe drought. After 1979, the drought intensity was moderate, which reflected the decrease in regional drought degree (Figure 5a). The change in P_j roughly reflects the change in drought coverage. In our study, in the past 56 years, the inter-annual P_j in Northwest China has varied greatly, fluctuating between 7.4% and 84.1% (Figure 5b). It showed an insignificant trend of first decreasing and then increasing, which indicated regional differences in drought occurrence. Before 1981, the P_j was greater than 50%, indicating that the Northwest region generally experienced regional drought during this period. In these years, the drought was moderate or above, while there were a few regional droughts in other periods. A total of 25, 18, 7, and 5 years of pan-regional drought, regional drought, partial region drought, and local drought occurred, respectively.

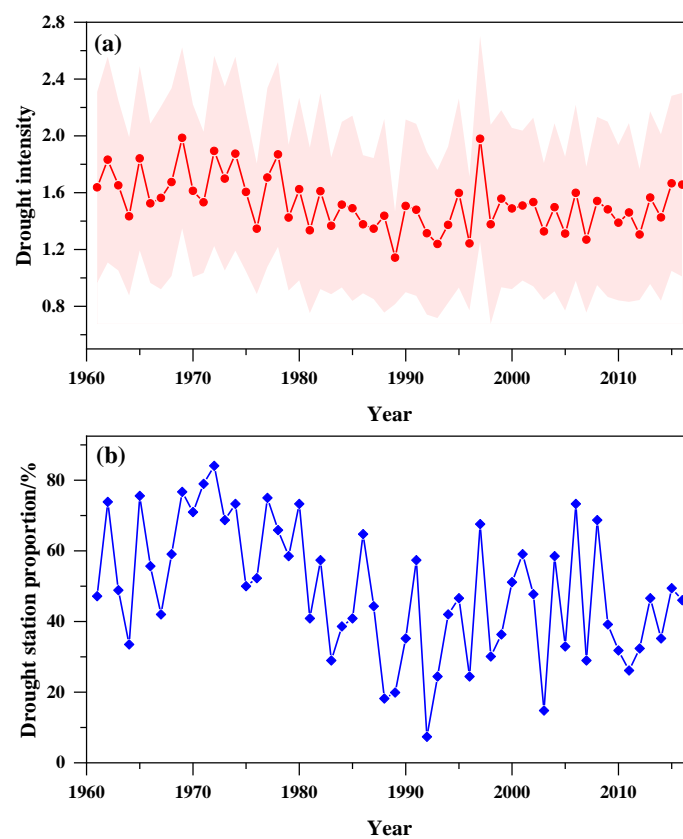


Figure 5. Variation of drought intensity (a) and drought station proportion (b) in Northwest China.

3.3.2. Periodicity of Annual SPEI and Drought

According to the wavelet analysis results of 56 years' SPEI values in Northwest China (Figure 6a), it was found that there were multiple time scales of 33–52, 11–19, and 4–7 years of SPEI in the entire time domain. In the study time domain, the 33–52 years' scale cycle oscillation was the most obvious, and it experienced 5 cycles of alternation between wet and dry. Meanwhile, the 12–19 years' scale and 4–7 years' scale cycle oscillations experienced 13 and 28 cycles of alternation between wet and dry, respectively. As the time scale decreased, the dry-wet alternations of SPEI became more frequent, and the corresponding climate abrupt points increased correspondingly. It is shown that SPEI did not change over a fixed time but in a nested form of three cycles of different lengths. According to the variation process of the 33–52 years' scale of SPEI, wet periods appeared in the early and middle 1960s, 1980s, early 1990s, and 2010s. The dry period occurred in the 1970s, late 1990s, and 2000s. The time distribution results of the wet and dry periods were consistent with the results of the average annual SPEI in Northwest China. Moreover, the changes in the

SPEI index in Northwest China in recent years were analyzed according to the wavelet analysis results of different time scales, and the results showed that the scale of 33–52 years tended to become wetter, while the time scale of 12–19 years and the time scale of 4–7 years both presented a drying trend. The large scale can reflect the inter-decadal background of drought change, while the small scale can reflect the detailed change of drought conditions under the large-scale background. Additionally, drought conditions exhibited increasingly complex periodic oscillations as time scales decreased.

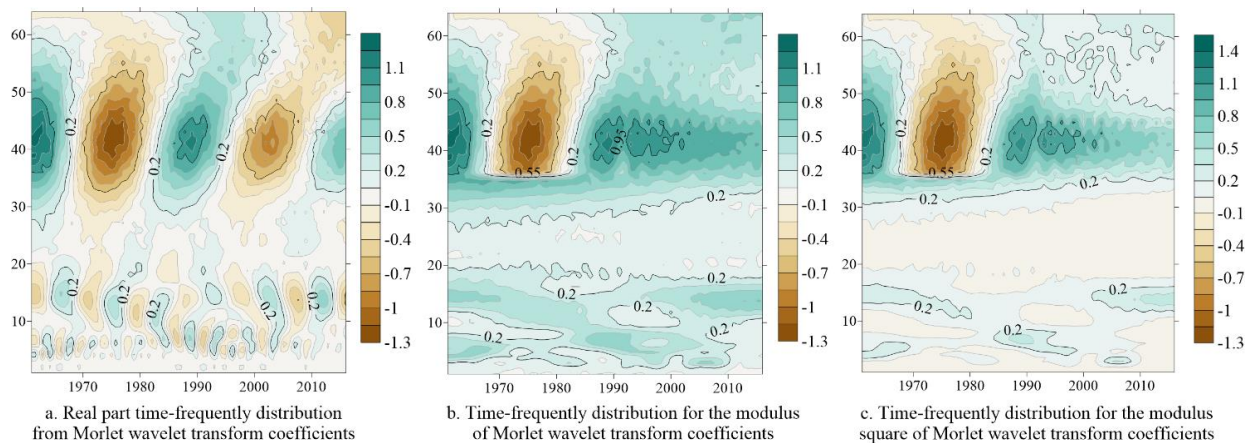


Figure 6. Results of Morlet wavelet transform for the annual SPEI in Northwest China.

The modulus of the wavelet coefficient could reflect the distribution of the energy density of different scale periods in the time domain. Additionally, the larger the modulus, the stronger the periodicity of the corresponding period or scale [37]. Meanwhile, the modulus square is similar to the wavelet energy spectrum, and the oscillation energy of different periods can be obtained [37]. According to the modulus and modulus square of the SPEI index wavelet transform (Figure 6b,c), it can be seen that the periodicity and signal strength of the annual SPEI in Northwest China were different on different time scales. The 33–52-year time scale had the strongest periodicity and the largest energy density, which was the main time scale affecting the SPEI index in this region in the future. Among them, the periodicity and energy of the 37–49-year time scale were the strongest, which were concentrated in the early 1960s to the 1980s. The periodicity of the 12–19-year time scale was the second, and the periodicity of 4–7 years was the least. Furthermore, the change in energy size corresponding to each time scale was consistent with the change of energy density. From large to small, the time scale was 33–52, 12–19, and 4–7 years.

As shown in Figure 7a, there were three peaks in the annual SPEI index time series in Northwest China in the past 56 years, and the variances corresponded to the time scales of 41, 14, and 6 years from the largest to the smallest. This is consistent with the time-frequency distribution of the real part, modulus, and modulus square of the wavelet transform coefficients. The results showed that the 41-year scale cycle had the strongest oscillation and was the first main cycle. The 14-year scale corresponded to the second peak, which was the second main cycle. Moreover, the third peak corresponded to the 6-year scale, which was the third main cycle. All these suggested that the variation characteristics of annual SPEI in the whole time domain were controlled by the above three periodic fluctuations.

To further explain the volatility characteristics of the alternating changes of annual SPEI values in Northwest China, the real part change process lines of the wavelet coefficients corresponding to the three main periods were drawn, as shown in Figure 7b–d. Similar to the conclusions of Lian et al. [38] and Zhang et al. [39], there were obvious mean cycle and dry-wet variation characteristics of drought conditions in Northwest China under different time scales. On a 41-year scale, the average cycle of drought change in Northwest China was about 28 years, with about 2 wet-dry transition periods (Figure 7b). On a 14-year scale,

the average period was about 9 years, and there were about 6 dry-wet changes. On a 6-year scale, the average period was about 4 years, with about 14 dry-wet changes. It can be seen that the SPEI index changed with the change of the main period scale in a long-period led by long-period oscillation superimposed, and the amplitude of different periods gradually decreased with the decrease of the main period scale. The corresponding phases of specific years on different time scales were different, indicating that the region was wet or dry in different periods, and the conclusions for specific years were different.

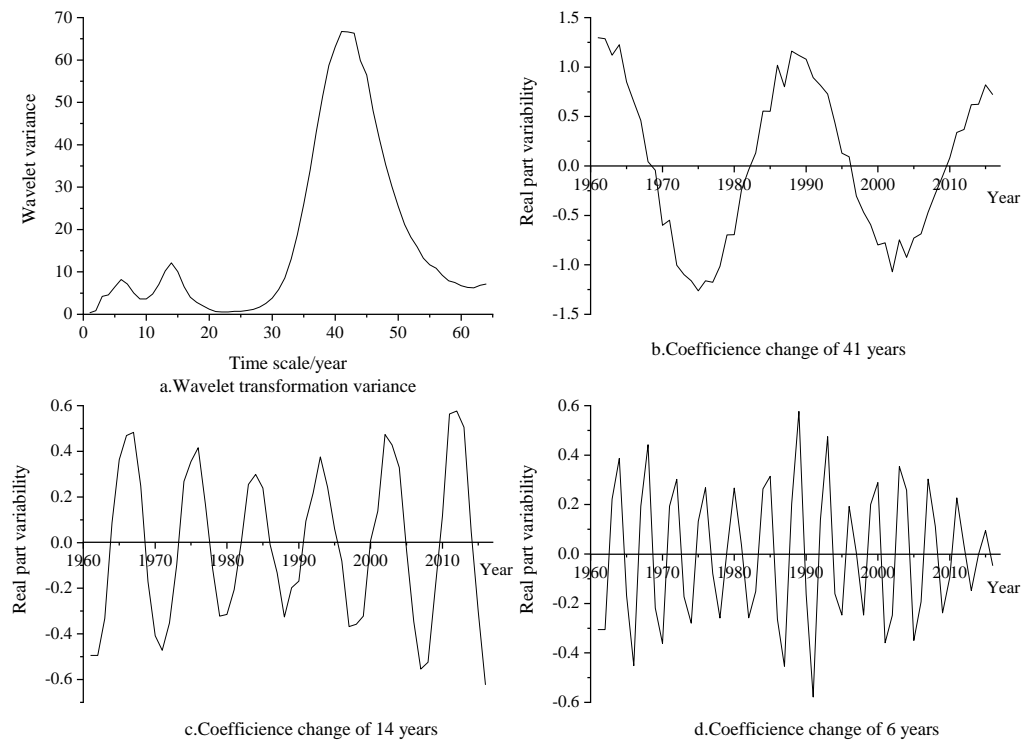


Figure 7. Wavelet transformation variance and specific real part of annual SPEI in Northwest China.

3.4. Shortage and Prospect of the Present Study

The present manuscript collected meteorological data up to 2017, not the latest year, which was a shortcoming of this article. On the other hand, this paper only discussed the changing trend of meteorological drought in Northwest China and did not explore the main factors that led to the evolution of meteorological drought. In fact, the atmospheric circulation and the influence of human activities may cause climate change [40,41], thus leading to a spatiotemporal difference in drought. The next research should focus on the factors affecting the meteorological drought in Northwest China and pay attention to the correlation between the influencing factors and climate change. Despite these limitations, the present research could investigate the drought characteristics for an exact period, including more recent or future seasons. Accordingly, the analysis of this study could be useful for coping with agricultural drought.

4. Conclusions

Based on the meteorological data from 1961 to 2017 in Northwest China, the SPEI index was calculated and the drought condition was analyzed. The results showed that the overall wetting and drying trend was slightly different on annual and seasonal scales in Northwest China. On a spring scale, the whole area showed a trend toward humidification. On a summer scale, a trend from wet to dry from northwest to southeast was observed in the whole area. On the autumn scale, except for a small part of the area, the whole area from northwest to southeast showed an obvious trend from wet to dry. On the winter scale, the distribution pattern of the whole region from northwest to southeast was from wet to dry and then to wet. Overall, the frequency of drought in Northwest China ranged from

large to small as moderate drought, extreme drought, severe drought, and light drought. Additionally, the whole area of Northwest China tended to humidify to different degrees, which would impact vegetation distribution and productivity and lead to changes in the irrigation schedule of crops. The drought intensity and drought station ratio showed varying degrees of fluctuation, according to the time analysis of the SPEI index. However, the trend of dry and wet in recent years, as well as the future dry and wet conditions of different regions in different periods, were not consistent. The 33–52-year time scale was the main time scale affecting the SPEI index in this region in the future based on the wavelet analysis. The results of our study can provide a reference for the efficient utilization of water resources, drought monitoring and early warning, drought prevention, and drought relief in Northwest China.

Author Contributions: Conceptualization, Y.P.; methodology, T.P.; software, Y.P. and Y.L.; validation, Y.L.; resources, Y.P.; data curation, Y.P.; writing—original draft preparation, Y.P.; writing—review and editing, T.P. and Y.L.; visualization, Y.P., T.P. and Y.L.; supervision, Y.L.; project administration, Y.L.; funding acquisition, Y.P. All authors have read and agreed to the published version of the manuscript.

Funding: This work was supported by the national science and technology programs (Grant No. E1230003).

Institutional Review Board Statement: Not applicable.

Informed Consent Statement: Not applicable.

Data Availability Statement: Not applicable.

Conflicts of Interest: The authors declare no conflict of interest.

References

- Samantaray, A.K.; Ramadas, M.; Panda, R.K. Changes in drought characteristics based on rainfall pattern drought index and the CMIP6 multi-model ensemble. *Agric. Water Manag.* **2022**, *266*, 107568. [[CrossRef](#)]
- Wu, Z.; Yu, L.; Du, Z.; Zhang, H.; Fan, X.; Lei, T. Recent changes in the drought of China from 1960 to 2014. *Int. J. Climatol.* **2020**, *40*, 3281–3296. [[CrossRef](#)]
- Hou, H.; Peng, S.; Xu, J.; Yang, S.; Mao, Z. Seasonal variations of CH₄ and N₂O emissions in response to water management of paddy fields located in southeast China. *Chemosphere* **2012**, *89*, 884–892. [[CrossRef](#)]
- Wu, M.; Li, Y.; Hu, W.; Yao, N.; Liu, D.L. Spatiotemporal variability of standardized precipitation evapotranspiration index in mainland china over 1961–2016. *Int. J. Climatol.* **2020**, *40*, 4781–4799. [[CrossRef](#)]
- Won, J.; Choi, J.; Lee, O.; Kim, S. Copula-based Joint Drought Index using SPI and EDDI and its application to climate change. *Sci. Total Environ.* **2020**, *744*, 140701. [[CrossRef](#)]
- Faiz, M.A.; Zhang, Y.; Zhang, X.; Ma, N.; Aryal, S.K.; Ha, T.T.V.; Baig, F.; Naz, F. A composite drought index developed for detecting large-scale drought characteristics. *J. Hydrol.* **2022**, *605*, 127308. [[CrossRef](#)]
- Ghasemi, P.; Karbasi, M.; Zamani Nouri, A.; Sarai Tabrizi, M.; Azamathulla, H.M. Application of Gaussian process regression to forecast multi-step ahead SPEI drought index. *Alex. Eng. J.* **2021**, *60*, 5375–5392. [[CrossRef](#)]
- Shi, X.; Yang, Y.; Ding, H.; Chen, F.; Shi, M. Analysis of the variability characteristics and applicability of SPEI in mainland China from 1985 to 2018. *Atmosphere* **2023**, *14*, 790. [[CrossRef](#)]
- Bae, S.; Lee, S.H.; Yoo, S.H.; Kim, T. Analysis of drought intensity and trends using the modified SPEI in south Korea from 1981 to 2010. *Water* **2018**, *10*, 327. [[CrossRef](#)]
- Yang, Y.; Gan, T.Y.; Tan, X. Spatiotemporal changes of drought characteristics and their dynamic drivers in Canada. *Atmos. Res.* **2020**, *232*, 104695. [[CrossRef](#)]
- Wu, J.; Tan, X.; Chen, X.; Lin, K. Dynamic changes of the dryness/wetness characteristics in the largest river basin of South China and their possible climate driving factors. *Atmos. Res.* **2020**, *232*, 104685. [[CrossRef](#)]
- Cao, S.; Zhang, L.; He, Y.; Zhang, Y.; Chen, Y.; Yao, S.; Yang, W.; Sun, Q. Effects and contributions of meteorological drought on agricultural drought under different climatic zones and vegetation types in Northwest China. *Sci. Total Environ.* **2022**, *821*, 153270. [[CrossRef](#)]
- Yang, P.; Zhang, S.; Xia, J.; Chen, Y.; Zhang, Y.; Cai, W.; Wang, W.; Wang, H.; Luo, X.; Chen, X. Risk assessment of water resource shortages in the Aksu River basin of northwest China under climate change. *J. Environ. Manag.* **2022**, *305*, 114394. [[CrossRef](#)] [[PubMed](#)]
- Jiang, Y.; Zhang, L.; Zhang, B.; He, C.; Jin, X.; Bai, X. Modeling irrigation management for water conservation by DSSAT-maize model in arid northwestern China. *Agr. Water Manag.* **2016**, *177*, 37–45. [[CrossRef](#)]
- Guo, G.; Yang, F.; Wu, R. Analysis on advantage of developing Melon crops with arched shed in Hetao area. *Inn. Mong. Agric. Sci. Technol.* **2015**, *43*, 127–128.

16. Chen, G.; Yang, G.; Zhao, M.; Wang, L.; Wang, Y.; Xue, J.; Gao, J.; Li, D.; Dong, S.; Li, C.; et al. Studies on maize small area super-high yield trails and cultivation technique. *J. Maize Sci.* **2008**, *16*, 1–4.
17. Tian, L.; Zhao, D.; Abdul, K.; Cui, J.; Xu, H.; Guo, R.; Lin, T. Climatic analysis of cotton region of Uzbekistan and Xinjiang. *Cotton Sci.* **2014**, *36*, 3–11.
18. Liu, H. Study on mechanism and regulation of soil water-salt-nutrient movement under drip irrigation of grape in saline land. *Shihezi Univ.* **2018**.
19. Liang, C.; Yu, S.; Zhang, H.; Wang, Z.; Li, F. Economic evaluation of drought resistance measures for maize seed production based on TOPSIS model and combination weighting optimization. *Water* **2022**, *14*, 3262. [[CrossRef](#)]
20. He, G.; Liu, H.; Wang, J.; Zhao, Y.; Zhu, Y.; Jiang, S.; Li, H.; Zhai, J.; He, F. Energy-water security challenge: Impact of energy production on water sustainable developments in Northwest China in 2017 and 2030. *Sci. Total Environ.* **2021**, *766*, 144606. [[CrossRef](#)]
21. Zhang, Q.; Yao, Y.; Li, Y.; Luo, Z.; Zhang, C.; Li, D.; Wang, R.; Wang, J.; Chen, T.; Xiao, G.; et al. Research progress and prospect on the monitoring and early warning and mitigation technology of meteorological drought disaster in northwest China. *Adv. Earth Sci.* **2015**, *30*, 196–213.
22. Alam, N.M.; Sharma, G.C.; Moreira, E.; Jana, C.; Mishra, P.K.; Sharma, N.K.; Mandal, D. Evaluation of drought using SPEI drought class transitions and log-linear models for different agro-ecological regions of India. *Phys. Chem. Earth* **2017**, *100*, 31–43. [[CrossRef](#)]
23. Zhang, X.; Pan, X.; Xu, L.; Wei, P.; Yin, Z.; Shao, C. Analysis of spatio-temporal distribution of drought characteristics based on SPEI in Inner Mongolia during 1960–2015. *Trans. Chin. Soc. Agric. Eng.* **2017**, *33*, 190–199.
24. Allen, R.G. Crop Evapotranspiration—Guidelines for computing crop water requirements. *Irrig. Drain. Ser.* **2006**, *56*, D05109.
25. Si, P.; Hao, L.; Luo, C.; Cao, X.; Liang, D. The interpolation and homogenization of long-term temperature time series at Baoding observation station in Hebei province. *Clim. Chang. Res.* **2017**, *13*, 41–51.
26. Yu, W. Construct meteorological similarity network and missing meteorological elements data interpolation. *Southwest Univ.* **2015**.
27. Huang, W.; Yang, X.; Li, M.; Zhang, X.; Wang, M.; Dai, S.; Ma, J. Evolution characteristics of seasonal drought in the south of China during the past 58 years based on standardized precipitation index. *Trans. Chin. Soc. Agric. Eng.* **2010**, *26*, 50–59.
28. Bera, B.; Shit, P.K.; Sengupta, N.; Saha, S.; Bhattacharjee, S. Trends and variability of drought in the extended part of Chhota Nagpur plateau (Singbhum Protocontinent), India applying SPI and SPEI indices. *Environ. Chall.* **2021**, *5*, 100310. [[CrossRef](#)]
29. Guna, A.; Zhang, J.; Tong, S.; Bao, Y.; Han, A.; Li, K. Effect of climate change on maize yield in the growing season: A case study of the Songliao Plain maize belt. *Water* **2019**, *11*, 2108. [[CrossRef](#)]
30. Cohen, E.A.K.; Walden, A.T. A Statistical Study of Temporally Smoothed Wavelet Coherence. *IEEE Trans. Signal Process.* **2010**, *58*, 2964–2973. [[CrossRef](#)]
31. Yang, F.; Wang, S.; Liu, X.; Shen, N. The Spatial interpolation and GeoDatabase foundation of average 10-day air temperature of Heilongjiang province in recent 10 years based on ArcGIS. *Heilongjiang Agric. Sci.* **2009**, *5*, 120–124.
32. Zhang, Q.; Zhu, B.; Yang, J.; Ma, P.; Liu, X.; Lu, G.; Wang, Y.; Yu, H.; Liu, W.; Wang, D. New characteristics about the climate humidification trend in Northwest China. *Chin. Sci. Bull.* **2021**, *66*, 3757–3771. [[CrossRef](#)]
33. Yang, P.; Xia, J.; Zhang, Y.; Wang, L. Drought assessment in Northwest China during 1960–2013 using the standardized precipitation index. *Clim. Res.* **2016**, *72*, 73–82. [[CrossRef](#)]
34. Liu, Y.; Mao, W.; Li, S.; Zhao, X.; Zhang, X.; Wu, H.; Su, X. Spatiotemporal evolution characteristics of meteorological droughts in northwest China. *J. Water Resour. Water Eng.* **2022**, *33*, 86–92.
35. Chen, F.; Xie, T.; Yang, Y.; Chen, S.; Chen, F.; Huang, W.; Chen, J. Discussion of the “warming and wetting” trend and its future variation in the drylands of Northwest China under global warming. *Sci. China Earth Sci.* **2023**, *66*, 1241–1257. [[CrossRef](#)]
36. Xu, H.; Wang, X.; Zhao, C.; Yang, X. Diverse responses of vegetation growth to meteorological drought across climate zones and land biomes in northern China from 1981 to 2014. *Agric. For. Meteorol.* **2018**, *262*, 1–13. [[CrossRef](#)]
37. Cao, S.; He, Y.; Zhang, L.; Chen, Y.; Yang, W.; Yao, S.; Sun, Q. Spatiotemporal characteristics of drought and its impact on vegetation in the vegetation region of Northwest China. *Ecol. Indic.* **2021**, *133*, 108420. [[CrossRef](#)]
38. Lian, L.; Liu, B. Change characteristics of dry and wet spells in northwest China during the past 58 years. *Arid Land Geogr.* **2019**, *42*, 1301–1309.
39. Zhang, Y.; Zhang, Y.; Cheng, L.; Cong, N.; Zheng, Z.; Huang, K.; Zhang, J.; Zhu, Y.; Gao, J.; Sun, Y. Have China’s drylands become wetting in the past 50 years? *J. Geogr. Sci.* **2023**, *33*, 99–120. [[CrossRef](#)]
40. Ye, H. The influence of air temperature and atmospheric circulation on winter fog frequency over Northern Eurasia. *Int. J. Climatol.* **2010**, *29*, 729–734. [[CrossRef](#)]
41. Lu, C.; Sun, Y.; Christidis, N.; Stott, P.A. Contribution of global warming and atmospheric circulation to the Hottest spring in Eastern China in 2018. *Adv. Atmos. Sci.* **2020**, *37*, 1285–1294. [[CrossRef](#)]

Disclaimer/Publisher’s Note: The statements, opinions and data contained in all publications are solely those of the individual author(s) and contributor(s) and not of MDPI and/or the editor(s). MDPI and/or the editor(s) disclaim responsibility for any injury to people or property resulting from any ideas, methods, instructions or products referred to in the content.